Supplementary Information

Table S1. Ionic radii for cation ions under corresponding coordination numbers.

Ion	Coordination number (CN)	Ionic radius (Å)
Ga^{3+}	6	0.62
Ge^{4+}	6	0.39
Zn^{2+}	6	0.74
Cr^{3+}	6	0.615

Table S2. Main parameters of processing and refinement of $CaZrTaGa_{1-2x}Ge_xZn_xO_7$:0.01$Cr^{3+}$ (x = 0-0.5).

Sample	x = 0	x = 0.1	x = 0.2	x = 0.3	x = 0.4	x = 0.5
Space group	*P2/c*	*P2/c*	*P2/c*	*P2/c*	*P2/c*	*P2/c*
a (Å)	12.7070	12.6966	12.6778	12.6826	12.6799	12.6759
b (Å)	7.3596	7.3322	7.3446	7.3506	7.3457	7.3489
c (Å)	11.4500	11.4182	11.4216	11.4276	11.4238	11.4264
V (Å^3)	1051.369	1044.772	1044.104	1046.009	1044.616	1045.133
β (º)	100.928	100.615	100.962	100.930	100.964	100.922
R_{wp} (%)	7.34	9.87	6.47	8.69	8.62	8.45
R_p (%)	5.37	5.89	4.37	6.23	5.87	6.75
χ^2	1.821	1.425	1.432	1.627	1.634	1.892

Table S3. Emission intensity ratio of 423 K and 298 K (I_{423}/I_{298}) and quantum efficiency (IQE and EQE) for some Cr^{3+}-doped phosphors with emission wavelength in 760-850 nm, as well as NIR output power and conversion efficiency of the corresponding fabricated *pc*-LEDs.

No.	Phosphor	λ_{em} (nm)	FWHM (nm)	IQE (%)	I_{423}/I_{298} (%)	Ref
1	$Na_3In_2Li_3F_{12}:Cr^{3+}$	778	121	33	44	[1]
2	$La_3Sc_2Ga_3O_{12}:Cr^{3+}$	818	145	35	60	[2]
3	$ScBO_3:Cr^{3+}$	800	120	65	51	[3]
4	$BaMgAl_{10}O_{17}:Cr^{3+}$	762	92.6	94	53	[4]
5	$GaTaO_4:Cr^{3+}$	850	266	82.6	73	[5]
6	$Ca_2LuZr_2Al_3O_{12}:Cr^{3+}$	780	117	69.1	60	[6]
7	$Gd_3Zn_{0.8}Ga_{3.4}Ge_{0.8}O_{12}: Cr^{3+}$	800	105	79.6	40.2	[7]
8	$Gd_3In_2Ga_3O_{12}:Cr^{3+}$	780	124	85.3	87.7	[8]
9	CZTGGZO: $0.01Cr^{3+}$ phosphor	812	250.39	94.37	88.56	This work
10	CZTGGZO: $0.01Cr^{3+}$ PiG film	812	248.37	90.20	92.34	This work

According to the Tanabe-Sugano plot, the energy level distribution of Cr^{3+} at octahedral positions is displayed. Therefore, the corresponding crystal field parameters of Cr^{3+} are calculated as follows (Figure S3)[9]:

$$D_q = \frac{E(^4T_2)}{10} \tag{S1}$$

$$B = D_q \frac{x^2 - 10x}{15(x-8)} \tag{S2}$$

$$x = \frac{E(^4T_1 - {}^4T_2)}{D_q} \tag{S3}$$

where D_q is the crystal field strength, B is the Racah parameter denoting the repulsive force between electrons in the three-dimensional orbitals, and E denotes the energy difference between the $^4T_1$ and $^4T_2$ energy levels determined by the positions of the $^4T_1(^4F)$ and $^4F_2(^4F)$ peaks. When x = 0.4 and D_q/B =2.9, it indicates that the octahedral site where Cr^{3+} is located favors broadband emission of Cr^{3+}.

The Kubelka-Munk equation is used to determine the band gap of the sample[2, 10]:

$$F(R) = \frac{(1-R)^2}{2R} \tag{S4}$$

$$Ah\nu = c(h\nu - E_g)^{\frac{1}{2}} \tag{S5}$$

$$[h\nu F(R_\infty)]^2 = A(h\nu - E_g) \tag{S6}$$

where E_g is the optical band gap, c is the absorption constant, $h\nu$ is the photon energy, and R is the reflection coefficient. The E_g value was calculated as 1.64 eV for CZTGO: 0.01Cr^{3+} as shown in Figure S2c.

The decay curves of the phosphor and PiG film monitored at 827 nm under 461 nm excitation can be fitted according to the following equations[11]:

$$I(t) = I_0 + A_1 \exp(-\frac{t}{t_1}) + A_2 \exp(-\frac{t}{t_2}) \tag{S7}$$

Where t is the time, A_1 and A_2 stand for constants, and $I(t)$ and I_0 represent the luminous intensity at times t and 0. Then, the lifetime of the luminescent center can be calculated by the following equation[11, 12]:

$$\tau = \frac{\int_0^\infty tI(t)dt}{\int_0^\infty I(t)dt} \tag{S8}$$

Where τ is the fluorescence lifetime.

Equation S9 fits the energy difference ΔE_a, as well as activation energy, between the lowest excited state and the crossover point location[13].

$$I_T = \frac{I_0}{1 + c * \exp(-\frac{E_a}{kT})} \tag{S9}$$

where C is a constant that is independent of temperature, k is the Boltzmann constant, and I_0 and I_t are, respectively, the starting and the intensity of luminescence at temperature T.

The luminescent spectra for QE measurement (S_1 part) were only recorded till 850 nm due to the range limitation of the instrument. The missing S_2 part (850–1100) should be taken into consideration for the actual IQE. Therefore, the actual IQE can be calculated via the following equation[14]:

$$IQE = IQE_m \times (S_1 + S_2) / S_1 \tag{S4}$$

where IQE and IQE_m are the actual IQE and measured IQE. S_1 (550–850 nm) and S_2 (850–1100 nm) are integrated intensities, which are obtained from PL spectra. The actual IQEs of $CaZrTaGa_{0.2}Ge_{0.4}Zn_{0.4}O_7$:0.01$Cr^{3+}$ phosphor and PiG film are determined to be 55.67% and 54.12%, respectively.

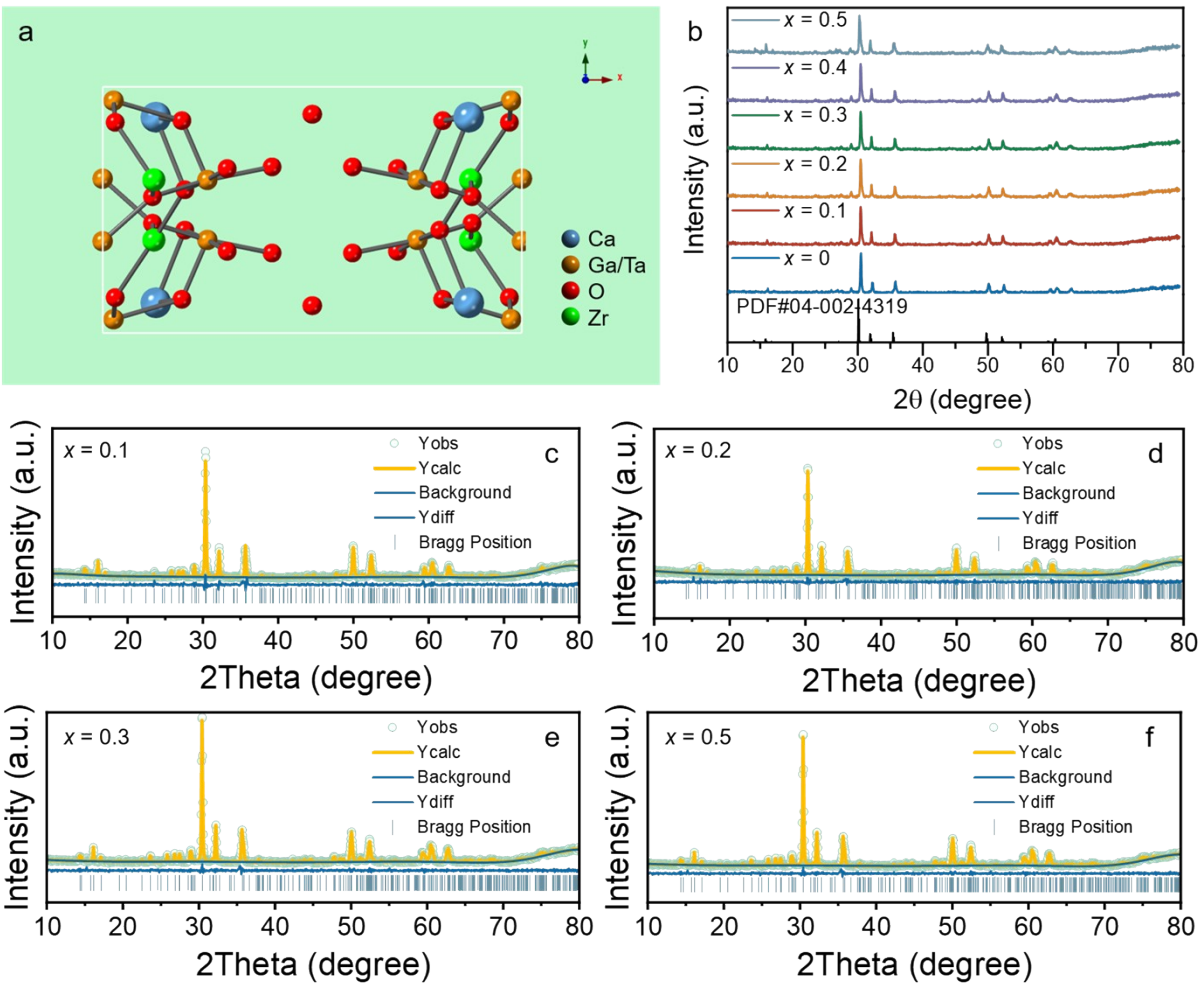

Figure S1. (a) Projection of the crystal structure of $CaZrTaGaO_7$ along the z axis. (b) XRD patterns of the $CaZrTaGa_{1-2x}Ge_xZn_xO_7$:0.01$Cr^{3+}$ samples (x = 0–0.5). (c) - (f) Rietveld refinement results of the synthesized $CaZrTaGa_{1-2x}Ge_xZn_xO_7$:0.01$Cr^{3+}$ (x = 0.1, 0.2, 0.3, 0.5).

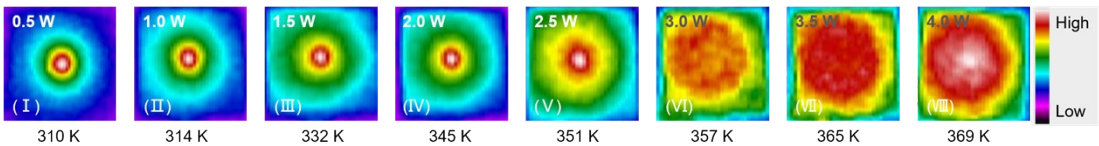

Figure S2. (d) Infrared thermal images of 20 s are taken at a laser power of 1-4 W under blue LD conditions.

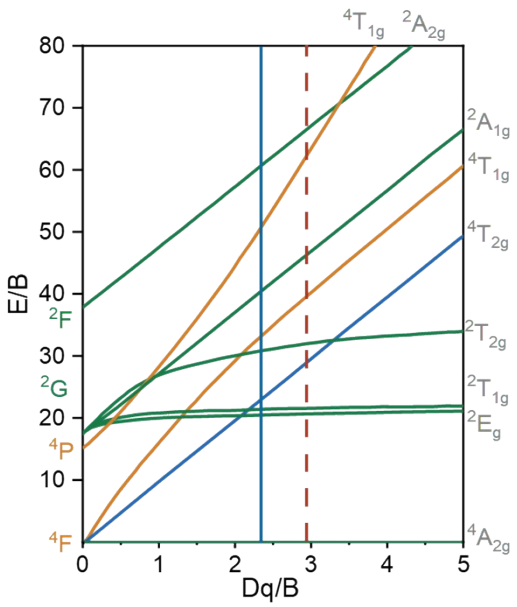

Figure S3. The Tanabe–Sugano diagram.

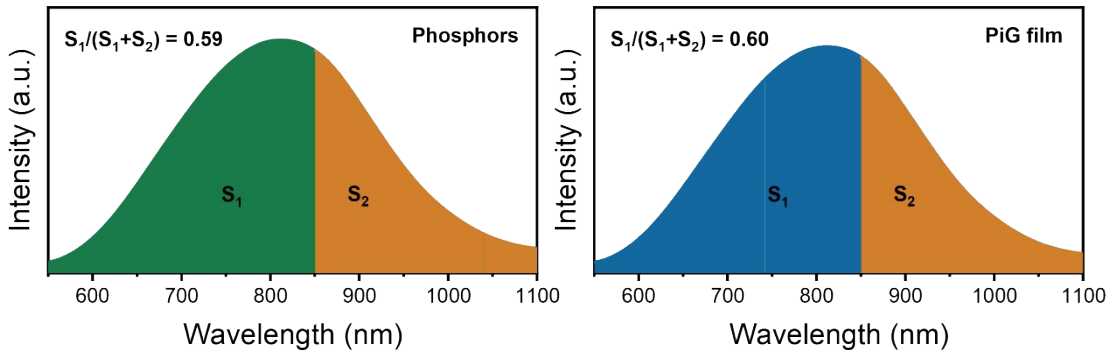

Figure S4. Comparison between IQE measuring spectra and PL spectra for $CaZrTaGa_{0.2}Ge_{0.4}Zn_{0.4}O_7$:0.01$Cr^{3+}$ phosphor and PiG film.

References

1. Nie, W.; Li, Y.; Zuo, J.; Kong, Y.; Zou, W.; Chen, G.; Peng, J.; Du, F.; Han, L.; Ye, X., Cr^{3+}-activated $Na_3X_2Li_3F_{12}$ (X = Al, Ga, or In) garnet phosphors with broadband NIR emission and high luminescence efficiency for potential biomedical application. *Journal of Materials Chemistry C* **2021,** *9* (42), 15230-15241.
2. Bai, B.; Dang, P.; Huang, D.; Lian, H.; Lin, J., Broadband Near-Infrared Emitting $Ca_2LuScGa_2Ge_2O_{12}:Cr^{3+}$ Phosphors: Luminescence Properties and Application in Light-Emitting Diodes. *Inorg Chem* **2020,** *59* (18), 13481-13488.
3. Shao, Q.; Ding, H.; Yao, L.; Xu, J.; Liang, C.; Jiang, J., Photoluminescence properties of a $ScBO_3:Cr^{3+}$ phosphor and its applications for broadband near-infrared LEDs. *RSC Advances* **2018,** *8* (22), 12035-12042.
4. You, L.; Tian, R.; Zhou, T.; Xie, R.-J., Broadband near-infrared phosphor $BaMgAl_{10}O_{17}:Cr^{3+}$ realized by crystallographic site engineering. *Chemical Engineering Journal* **2021,** *417*, 129224.
5. Zhong, J.; Zhuo, Y.; Du, F.; Zhang, H.; Zhao, W.; You, S.; Brgoch, J., Efficient Broadband Near‐Infrared Emission in the $GaTaO_4:Cr^{3+}$ Phosphor. *Advanced Optical Materials* **2021,** *10* (2), 2101800.
6. Zhang, L.; Zhang, S.; Hao, Z.; Zhang, X.; Pan, G.-h.; Luo, Y.; Wu, H.; Zhang, J., A high efficiency broad-band near-infrared $Ca_2LuZr_2Al_3O_{12}:Cr^{3+}$ garnet phosphor for blue LED chips. *Journal of Materials Chemistry C* **2018,** *6* (18), 4967-4976.
7. Wang, Y.; Wang, Z.; Wei, G.; Yang, Y.; He, S.; Li, J.; Shi, Y.; Li, R.; Zhang, J.; Li, P., Ultra-Broadband and high efficiency Near-Infrared $Gd_3Zn_xGa_{5-2x}Ge_x O_{12}:Cr^{3+}$ (x = 0–2.0) garnet phosphors via crystal field engineering. *Chemical Engineering Journal* **2022,** *437*, 135346.
8. Li, C.; Zhong, J.; Jiang, H.; Shi, P., Efficient and thermally stable broadband near-infrared emission in a garnet $Gd_3In_2Ga_3O_{12}:Cr^{3+}$ phosphor. *Dalton Transactions* **2022,** *51* (43), 16757-16763.
9. Liu, G.; Molokeev, M. S.; Lei, B.; Xia, Z., Two-site Cr^{3+} occupation in the $MgTa_2O_6:Cr^{3+}$ phosphor toward broad-band near-infrared emission for vessel visualization. *Journal of Materials Chemistry C* **2020,** *8* (27), 9322-9328.
10. Shi, R.; Miao, S.; Zhang, Y.; Lv, X.; Chen, D.; Liang, Y., Blue-light-excitable pure and efficient short-wave infrared luminescenceviaCr^{3+}→Yb^{3+} energy transfer in a $KYbP_2O_7:Cr^{3+}$phosphor. *Journal of Materials Chemistry C* **2023,** *11* (7), 2748-2755.
11. Jin, Y.; Zhou, Z.; Ran, R.; Tan, S.; Liu, Y.; Zheng, J.; Xiang, G.; Ma, L.; Wang, X. j., Broadband NIR Phosphor $Ca_2LuScAl_2Si_2O_{12}:Cr^{3+}$ for NIR LED Applications. *Advanced Optical Materials* **2022,** *10* (24), 2202049.

12. Zhong, J.; Zhuo, Y.; Du, F.; Zhang, H.; Zhao, W.; Brgoch, J., Efficient and Tunable Luminescence in $Ga_{2-x}In_xO_3:Cr^{3+}$ for Near-Infrared Imaging. *ACS Appl Mater Interfaces* **2021,** *13* (27), 31835-31842.
13. Zeng, H.; Zhou, T.; Wang, L.; Xie, R.-J., Two-Site Occupation for Exploring Ultra-Broadband Near-Infrared Phosphor-Double-Perovskite La2MgZrO6:Cr3+. *Chemistry of Materials* **2019,** *31* (14), 5245-5253.
14. Liu, D.; Li, G.; Dang, P.; Zhang, Q.; Wei, Y.; Qiu, L.; Lian, H.; Shang, M.; Lin, J., Valence conversion and site reconstruction in near-infrared-emitting chromium-activated garnet for simultaneous enhancement of quantum efficiency and thermal stability. *Light Sci Appl* **2023,** *12* (1), 248.